



Effect of Modified Clay on the Morphological and Thermal Properties of Poly lactic acid, Poly butylene adipate-co-terephthalate Nanocomposites

MOHD JUNAEDY OSMAN^{1*}, NOR AZOWA IBRAHIM² and WAN MD ZIN WANYUNUS³

¹Department of Chemistry and Biology, Center for Defence Foundation Studies, Universiti Pertahanan Nasional Malaysia, Kem Sungai Besi, 57000 Kuala Lumpur, Malaysia.

²Chemistry Department, Faculty of Science, Universiti Putra Malaysia, 43400 Serdang Selangor, Malaysia.

³Faculty of Defence Science and Technology, Universiti Pertahanan Nasional Malaysia, Kem Sungai Besi, 57000 Kuala Lumpur, Malaysia.

*Corresponding author E-mail: mohdjunaedy@gmail.com

<http://dx.doi.org/10.13005/ojc/330639>

(Received: August 29, 2017; Accepted: September 26, 2017)

ABSTRACT

In this study, new biodegradable polylactic acid/poly butylene adipate-co-terephthalate nanocomposites were developed and prepared using the melt blending method. Sodium montmorillonite clay was modified using organic surfactant, octadecyl ammonium bromide, novel dimethyl dioctadecyl ammonium bromide. A commercial organomodified montmorillonite, Cloisite 20A was also used as comparison. Increased interlayer spacing, reduced free water molecule within montmorillonite clay gallery spacing and existence of alkyl group signature confirmed that organomodified montmorillonite was successfully prepared via ion exchange technique. The present work introduced 1% organomodified montmorillonite into PLA/PBAT blends. Surface morphology improved with addition of OMMT. Transition electron microscope analysis revealed exfoliated distribution between the organoclay and the matrix. The onset temperature (T_{onset}) increased after the addition of organoclay.

Keywords: Poly lactic acid (PLA), Poly butylene adipate-co-terephthalate (PBAT), Organomodified montmorillonite (OMMT), Morphological properties, Thermal properties.

INTRODUCTION

Poly lactic acid (PLA) is the most popular biodegradable polymers obtained from corn starch¹. Standard-grade PLA has a high modulus and a strength, which is comparable to that of many petroleum-based plastics. Some disturbing properties of PLA such as its brittleness, low heat

distortion temperature, high gas permeability and low melt viscosity limit its uses in a wide range of application¹.

A plasticiser was used to improve its processability, flexibility and ductility². A new polymer, such as poly butylene adipate-co-terephthalate (PBAT), was used to modify the

properties of PLA by copolymerisation of lactide linkages available in PLA was observed to be a suitable substitute for this role. Addition of plasticizer bring up a new problem involving the compatibility of both polymer matrix. As a result, properties of the polymer blends produced worsen. Previous studies have revealed that PLA and PBAT blends are immiscible by consisting of two phases that can be observed using SEM. The debonding of round PBAT particles from the PLA matrix under tensile stress provides evidence that PLA/PBAT form immiscible blends caused by the weak interactions between both polymers³. Therefore, polymer blends tend to exhibit deterioration in their mechanical properties.

Immiscibility of polymer occur due to large interfacial tension between polymer matrixes⁴. Introduction of compatibilising agent to the polymer blends is one method to overcome this issue. Compatibilisers not only can reduce the interfacial tension between the immiscible polymer blends, but also increases the adhesion at phase boundaries in the polymer blends, which leads to a fine dispersion and improving the morphological and thermal properties of the final product⁵.

Among available compatibiliser, montmorillonite clay (MMT) is one of the compatibiliser that exist naturally and abundantly available. The development of polymer-layered silicate nanocomposites has recently attracted significant research interests, and these nanocomposites are considered one of the effective means for improving the properties of polymers⁶. The structure of clay was observed to consist of a silicate multilayer that can easily break down to form nanosized layers is the main reason for its vast industrial application as reinforcing fillers in polymer matrixes⁶.

Although promising properties of MMT, hydrophilic character of MMT prevent it from improving compatibility with organic polymer. In this research, sodium montmorillonite (Na-MMT) undergo ion exchange technique to replace inorganic cation by organic cation thus transform hydrophilic character of MMT to organophilic character. This technique will also increase the spacing between the silicate layers which in turn promote the fine dispersion for polymer matrixes.

Based on the above advancements and understanding, in this study, the OMMT was prepared using ODA, DDOA as the surfactant and introduced into the polymer blends to improve the interaction between both PLA and PBAT. Closite-20A was the commercial OMMT that was also used for comparison.

MATERIALS AND METHOD

In this study, PLA 4042D and PBAT (Ecoflex FBX 7011) were acquired from USA Nature works LLC, Minnetonka USA and BASF Plastic Technologies USA. Sodium montmorillonite (Na-MMT) with a cation exchange capacity of 119 meq/100 g clay was obtained from Kunimine Ind. Co., Japan. Octadecyl ammonium bromide (ODAB) was purchased from Merck Schuchardt OHG, Hohenbrunn, Germany and dimethyl dioctadecyl ammonium bromide (DDOAB) was purchased from Acros Organic, New Jersey, USA were used as an organic surfactant. The commercialised clay used was Closite 20A (C20A) from Southern Clay, USA.

Preparation of Organomodified MMT (OMMT)

Organomodified MMT was prepared through an ion-exchange technique. Na-MMT was slowly dispersed in the hot distilled water with continuous stirring for 1 h at 80°C. Next, surfactant suspension was poured into the hot montmorillonite dispersion and continuously stirring for 1 hour. The resultant white precipitate was collected via filtration by suction. The precipitate was then washed with hot distilled water by stirring for 1 h at 80°C. This process was repeated until no bromide ion was detected in the filtrate using 0.1 N AgNO₃ as the indicator. Then the organomodified montmorillonite (OMMT) was dried in the vent oven at 60°C for 24 h and was grinded in the mortar and sieved into 75 µm size. It was stored in the airtight bottle to prevent moisture absorption. The product was labeled as ODA-MMT. A similar method was performed to prepare the DDOA-MMT

Preparation of PLA/PBAT nanocomposites

All starting materials were dried before weighing. The materials were premixed before undergoing melt blending process. Premixed material were loaded into a Brabender internal mixer, mixing chamber, which was already heated

and stabilised at 180°C. Blending process occurred at 180°C using a 50 rpm rotor speed for 6 minutes. The resultant nanocomposites were then moulded by preheating the sample at 180°C for 2 min. followed by full pressing at 110 kg/cm² for 8 min. and cooling to room temperature for 8 min. under the same pressure to produce a sample sheet with dimensions of 150 x 150 x 1 mm³.

Characterisation and measurements

X-Ray Diffraction (XRD) Analysis

XRD analysis was used to investigate the interlayer spacing of the samples. The XRD data were obtained using a Shimadzu D-600 Diffractometer with an X-ray beam using nickel-filtered CuK α ($\lambda = 1.542 \text{ \AA}$) radiation operated at 30 kV and 30 mA. The continuous scanning rate was set at 1°/min. from 2° to 10°. Silica powder ($2\theta = 28.4229 \text{ \AA}$) was used in the calibration of this equipment.

Fourier Transform Infrared spectroscopy (FTIR)

FTIR analysis was carried out using

Fourier Transform Infra-Red Perkin Elmer 100. It was carried out with attenuated total reflectance (ATR) method. Infrared recorded at wavenumber range between 280 cm⁻¹ and 4000 cm⁻¹ at room temperature.

Scanning Electron Microscopy (SEM)

The morphology of tensile fractured surface of PLA/PBAT blends and PLA/PBAT nanocomposites was investigated using SEM, JOEL 4200 model at 500x magnification and operated at 20 kV to 30 kV. The samples were coated with gold using Polaron Equipment Unit E 1500.

Transmission Electron Microscopy (TEM)

The nanoscale structure of the nanocomposites was investigated using a high-resolution TEM (Hitachi H-7100) operated at an accelerating voltage of 100 kV. The ultrathin sample was prepared by dissolving 0.50 g of the nanocomposite in 100 ml chloroform and then

Table 1: Chemical structure of respective surfactant

Surfactant	Chemical structure
Octadecyl ammonium bromide (ODAB)	$\text{Br}^- \text{H}_2\text{N}^+(\text{CH}_2)_{17}\text{CH}_3$
Dimethyl diodecyl ammonium bromide (DDOAB)	$\text{Br}^- \text{CH}_3 \text{N}^+(\text{CH}_2)_{17}\text{CH}_3 \text{CH}_3$
Closite 20 A (C20A)	$\text{CH}_3 \text{N}^+(\text{HT})_2 \text{CH}_3$

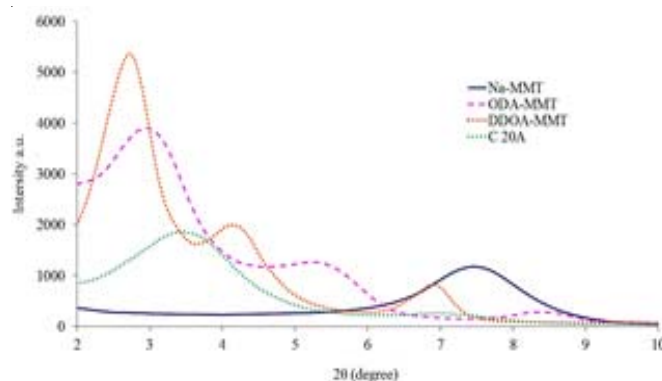


Fig. 1. XRD patterns for Na-MMT and OMMT

transferring one drop of the dissolved solution onto the 200-mesh copper grids.

Thermogravimetric Analysis

Thermal analysis of sample was performed using a Perkin Elmer TGA 7 thermal analyser. Approximately 3.0 mg of the nanocomposites was heated from 35°C to 800°C at a heating rate of 10°C/min. The analysis was performed under a nitrogen atmosphere with a nitrogen flow rate of 20 ml/min. The weight loss of the sample during heating was recorded and plotted as a function of time.

RESULTS AND DISCUSSION

Clay Modification

XRD analysis

The purpose of ion exchange procedure using surfactant was to make the hydrophilic Na-MMT more organophilic and to increase the interlayer spacing of Na-MMT to provide better physical and chemical environments for the nanocomposites. Increased interlayer spacing was confirmed via XRD analysis. The XRD peak position using the Bragg equation:

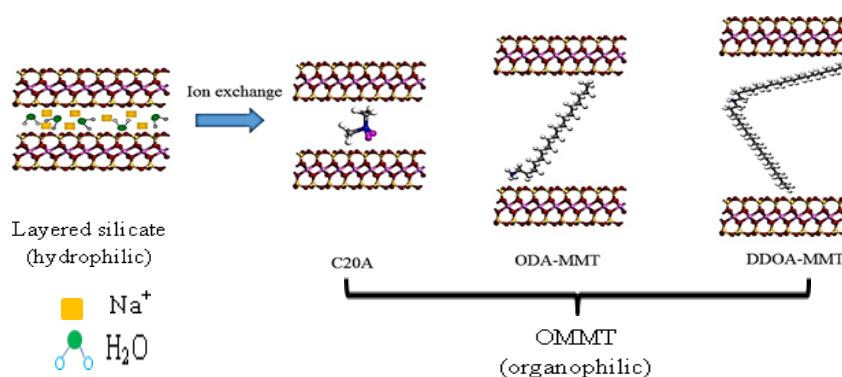


Fig. 2. Schematic of ion exchange in interlayer silicate

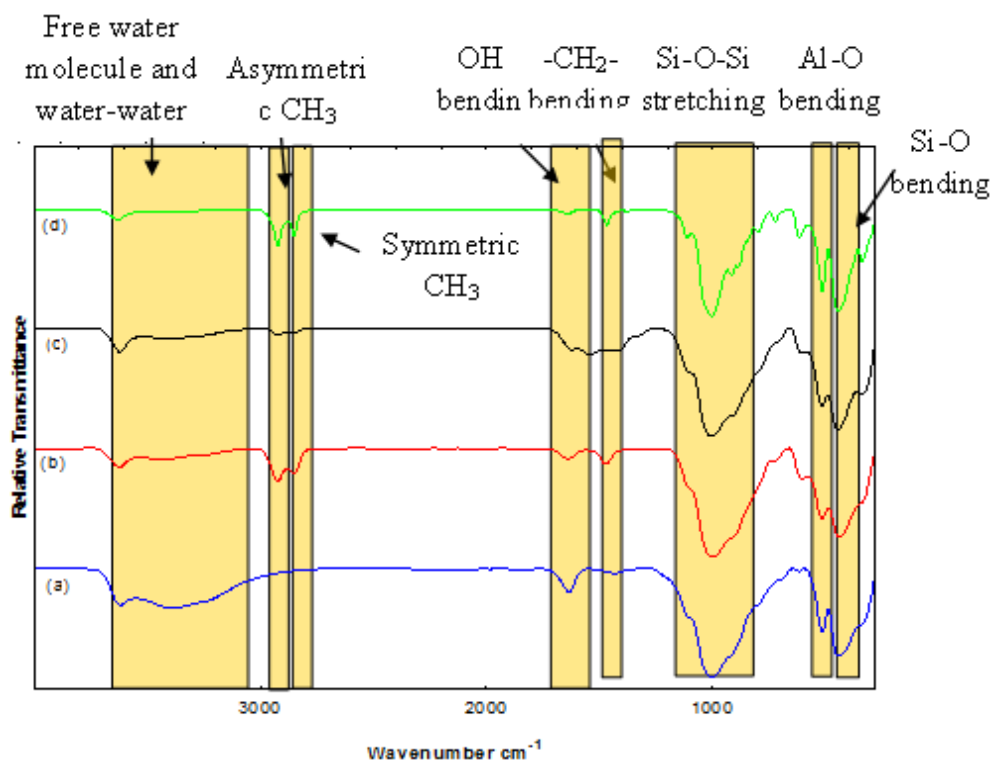


Fig. 3. FTIR spectra for (a) Na-MMT, (b) ODA-MMT, (c) DDOA-MMT and (d) C20A

$$d = \frac{n\lambda}{2\sin\theta} \quad \text{--(1)}$$

where d is the distance between the crystal planes or the interlayer spacing of the clay, n is a simple whole number ($n = 1$), λ is the wavelength of the X-ray used ($\lambda = 1.542 \text{ \AA}$) and θ is the angle of

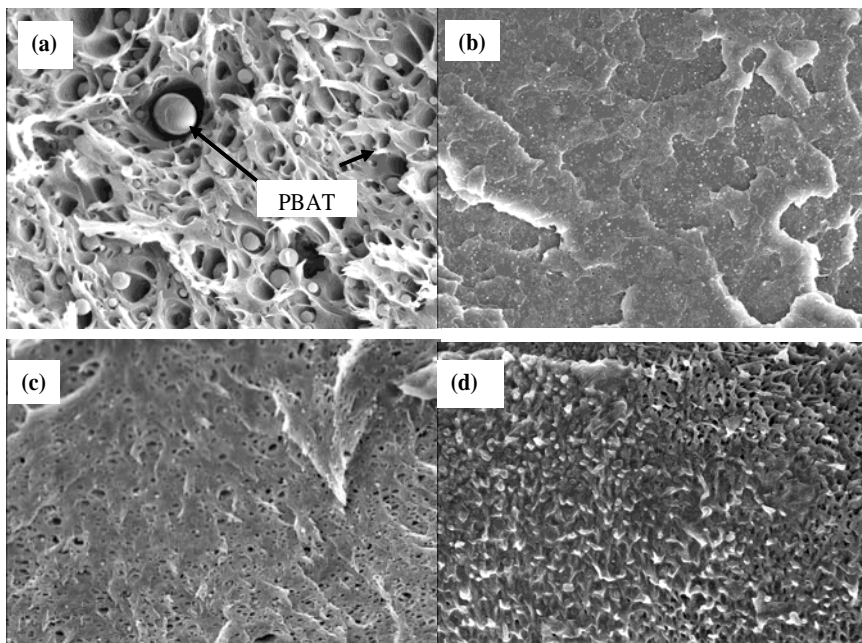


Fig. 4. SEM images of (a) PLA/PBAT blends, (b) PLA/PBAT/ODA-MMT, (c) PLA/PBAT/DDOA-MMT and (d) PLA/PBAT/C20A

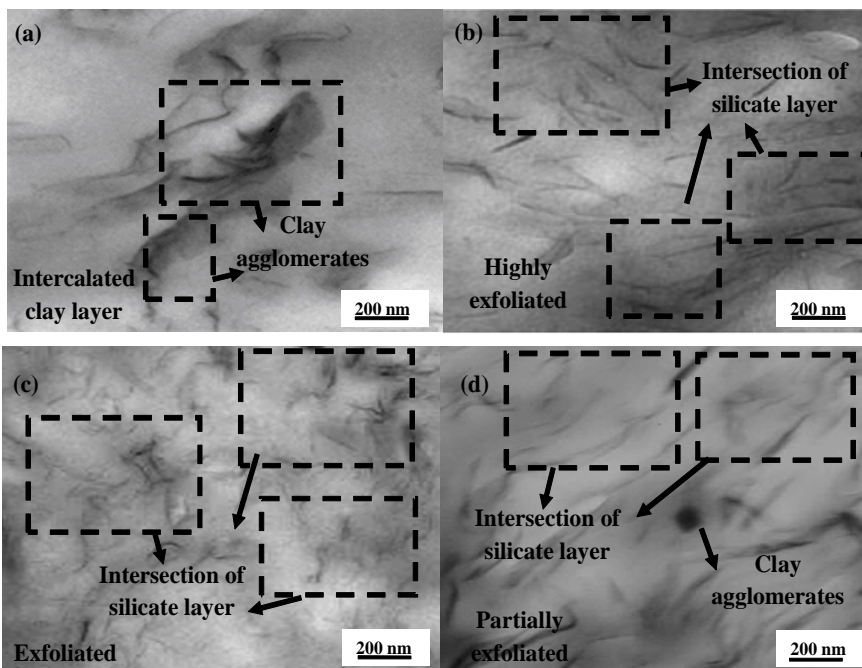


Fig. 5. TEM images for (a) PLA/PBAT/Na-MMT, (b) PLA/PBAT/ODA-MMT, (c) PLA/PBAT/DDOA-MMT and (d) PLA/PBAT/C20A nanocomposite

incidence of the rays. Fig. 1 represent XRD peak position of Na-MMT and various OMMT prepared. Observed that the peak position differ according to the sample. The interlayer spacing distance increases (from 11.85 Å to DDOA = 33.22 Å, ODA = 30.26 Å and C20A = 26.00 Å).

This trend was similar to the number of alkyl groups (DDOA = 38, ODA = 18 and C20A = 2) present for each surfactant used. The increased interlayer spacing indicates that the hydrated Na⁺ has been successfully exchanged with ODA⁺, DDOA⁺ and C 20A⁺ into the silicate layers⁷, as illustrated in Figure. 2.

FTIR analysis

FTIR analysis (Fig. 3) was to confirm the present of organic surfactant within interlayer

spacing of MMT and to identify the properties of prepared OMMT. The common features in the spectra of the natural Na-MMT and organoclay (ODA-MMT, DDOA-MMT and C20A) are the presence of band about 3638 cm⁻¹, 3442 cm⁻¹ and 1652 cm⁻¹ due to the free water molecules or weakly hydrogen-bonded water molecule to the surface oxygen of tetrahedral sheet, water-water hydrogen bond (Mn+-O-H-O-H) and OH (bending) vibration respectively. In addition, the decrement in intensity of free OH and OH (hydrogen bond) bands show that the organoclay become more organophilic. Interestingly to note that the appearance of three new peaks at 2920 cm⁻¹, 2852 cm⁻¹ and 1470 cm⁻¹ for OMMT which due to the stretching vibration of asymmetrical CH₃, symmetrical CH₃ stretching and -CH₂- scissor vibration band (methylene's bending) respectively. The presence of transmittance band

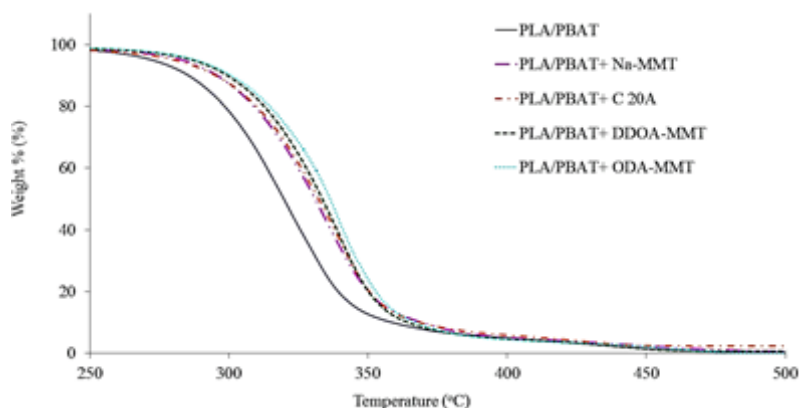


Fig. 6. TGA curve of sample nanocomposites

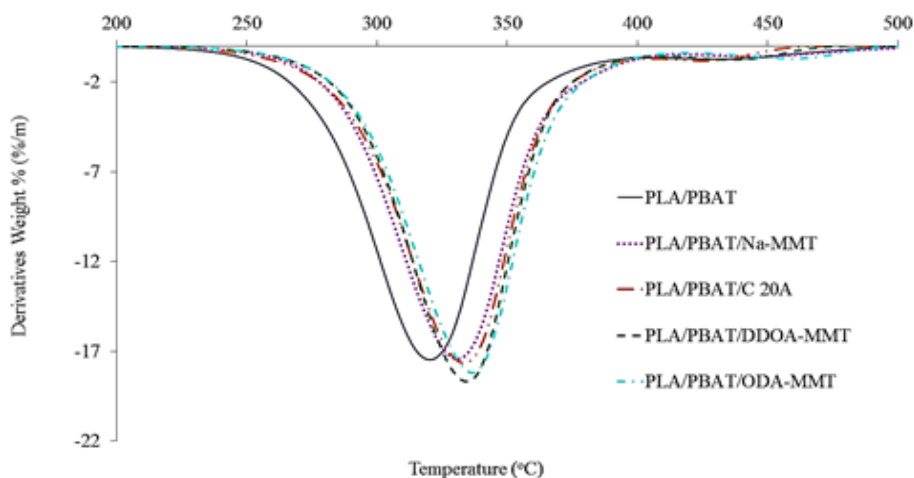


Fig. 7. DTG curve of sample nanocomposite

due to CH₃ and CH₂ in all organomodified and the reduced in intensity of free water molecules convey a strong evidence that MMT was successfully undergo ion exchange process⁸.

PLA/PBAT nanocomposites

Morphological study

The micrograph of fractured surface of 85:15 PLA/PBAT blends is shown at 1000x magnification (Fig. 4(a)). The micrograph reveals two phases as the blends are immiscible. The debonding of the round PBAT particles from the PLA matrix under tensile stress is clearly observed³. Note that the PLA samples are pulled apart as the appearances of cavities indicating the low adhesive properties between polymers. These cavities were formed during tension when the stress was higher than the bonding strength at the interface between the PLA matrix and PBAT inclusions. Because there was not sufficient interfacial adhesion (weak interaction) between PLA and PBAT, instead of cavitation's within the PBAT core under the stress, interfacial debonding took place³.

Introduction of OMMT into PLA/PBAT blends presents a good level of dispersion (Fig. 4 (b), (c) and (d)). The separated surfaces were not clearly seen and the diameter of cavities was also decreased. In addition, OMMT acts as a compatibiliser by absorbing PLA and/or PBAT on its surface resulting solid particles migration at the interface between the two polymeric phases and a good level of dispersion achieved⁹. The entire images indicating localized plastic deformation and this indicates that the nanocomposites may have some degree of toughness¹⁰ in comparison of pure PLA/PBAT.

The improved interface between OMMT and PLA/PBAT blends was further confirmed by TEM micrographs (Figure. 5).

TEM analysis

The dark lines represent the intersection of silicate layers, while the grey background corresponds to the PLA/PBAT matrix. From the images, PLA/PBAT/Na-MMT exhibits poor dispersion of clay platelets, where an intercalated clay layer stack can be observed in addition to the large clay agglomerates. This finding may be attributed to the presence of strong electrostatic forces between the clay layers¹¹.

The absence of aggregates confirms the high exfoliation of the layer silicate with the addition of OMMT. The increase in the number of alkyl groups of OMMT results in an increase in the interlayer spacing. The larger initial layer spacing may lead to easier exfoliation because platelet-platelet attraction is reduced¹². Interestingly to note that addition of ODA-MMT leads to a higher degree of exfoliated. This situation implies the diffusion of polymer chains inside clay galleries is less hindered eventually leads to improved exfoliation¹³.

Thermal Analysis

Thermal analysis of the sample was performed using TGA. Different types of nanoclay yield different thermal stability of the PLA/PBAT nanocomposites (Fig. 6). The 50% decomposition temperature (T_{50}) of PLA/PBAT, PLA/PBAT/ODA-MMT, PLA/PBAT/DDOA-MMT, PLA/PBAT/C 20A and PLA/PBAT/Na-MMT was 318.78°C, 336.09°C, 334.19°C, 332.13°C and 325.27°C, respectively. Based on these results, the onset temperature (T_{onset}) and the maximum decomposition temperature (T_{max}) also increased following the

Table 2: Thermal degradation of sample nanocomposites

Sample	T_{onset} (°C)	T_{50} (°C)	T_{max} (°C)
PLA/PBAT	275	319	322
PLA/PBAT/Na-MMT	287	325	329
PLA/PBAT/ C 20A	300	332	335
PLA/PBAT/DDOA-MMT	308	334	335
PLA/PBAT/ ODA-MMT	310	336	337

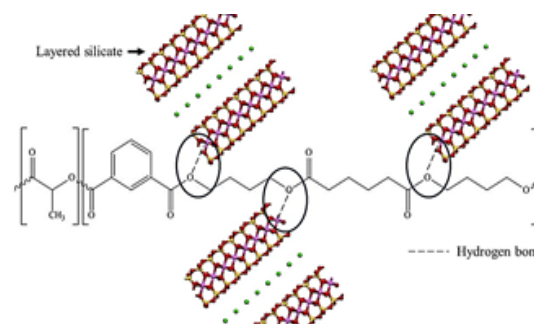


Fig. 8. Expected hydrogen bond formation between OMMT and PLA/PBAT blends

trend Na-MMT < C 20A < DDOA-MMT < ODA-MMT, as demonstrated in Table 2. The improvement can be clearly observed in the DTG result (Figure. 7).

The TGA curve demonstrates that the incorporation of clay into PLA/PBAT improves its thermal stability. Addition of OMMT additions increased the initial decomposition temperature compared with the pristine PLA/PBAT due to the reduced permeability oxygen and volatile biodegradation product resulting from the homogenous distribution of the OMMT particle barrier effect of these high aspect ratios and char formation¹⁴.

The decomposition of the PLA/PBAT nanocomposites at high temperature resulted from the "labyrinth" effect of the OMMT platelets dispersed on the nanometre scale in the PLA/PBAT, which was caused by strong interaction¹⁵ between OMMT platelets and PLA/PBAT. This process required more heat to break the bonding between PLA/PBAT/OMMT compared with the other nanocomposites.

Hydrogen Bond phenomenon

The introduction of modified clay into the PLA/PBAT was made to improve the properties of the blends. The hydrogen bond was suspected from the interaction between hydroxyl group from the interlayer galleries of the clay and the PLA/PBAT blends. Fig. 8. showed the expected formation of hydrogen bond between OMMT and PLA/PBAT blends.

This hydrogen bond increases the internal strength of PLA/PBAT/OMMT nanocomposites compared to neat PLA/PBAT. The increment in

internal strength may affected the morphology and thermal properties of sample. A larger interlayer spacing make hydroxyl group more exposed for hydrogen bond formation.

CONCLUSIONS

Improve in morphological and thermal stability coincided well with two factors: the internal strength of the materials and the gallery spacing of the OMMT. The addition of OMMT significantly enhanced the morphological and thermal properties of the PLA/PBAT blends. This mainly because there's strong intermolecular force between PLA/PBAT and OMMT. Favourable interactions between the surface of OMMT and better dispersion between PLA/PBAT and OMMT also contribute to this improvement. Modification of Na-MMT not only increase interlayer spacing of Na-MMT but also changed the characteristic of Na-MMT to be more organophilic which provide better physical and chemical environments for the nanocomposites. A fine dispersion of OMMT within polymer matrices leads to considerable improvement of morphology and thermal properties compared with the neat polymer blends, which broadens the application field of these biopolymers.

ACKNOWLEDGEMENTS

The author would like to thank the Ministry of Higher Education of Malaysia (Research Acculturation Collaborative Effort (RACE/F3/ST5/UPNM/1), Universiti Pertahanan Nasional Malaysia, Universiti Putra Malaysia and Malaysian Nuclear Agency for the financial support and facility for this research.

REFERENCES

1. Mohamad Haafiza, M.K.; Hassana, A.; Zakariac, Z.; Inuwaa, I.M.; Islamd, M.S.; Jawaide, M. *Carbohydr. Polym.* **2013**, *98*, 139 – 145.
2. Burgos, N.; Veronica, P.M.; Jimenez, A. *Polym. Degrad. Stab.* **2013**, *98*, 651 – 658.
3. Jiang, L.; Wolcott, M.P.; Zhang, J. (2006). *Biomacromolecules*. **2006**, *7*(1), 199 – 207.
4. Tagueta, A.; Cassagnaub, P.; Lopez-Cuestaaa, J.M. *Prog. Polym. Sci.* **2014**, *39*, 1526 – 1563.
5. Wang, P.; Ma, J.; Wang, Z.; Shi, F.; Liu, Q.

- Langmuir*. **2012**, *28*, 4776 – 4786.
6. Lin, J.J.; Chan, Y.N.; Lan, Y.F. *Materials*. **2010**, *3*, 2588 – 2605.
 7. Singla, P.; Mehta, R.; Upadhyay, S.N. *Green Sustain. Chem*. **2012**, *2*, 21 – 25.
 8. Karaca, S.; Gürses, A.; Korucu, M. E. *J. Chem*. **2013**, 1 – 10.
 9. Shiraz, N. Z.; Enferad, E.; Monfared, A.; and Mojarrad, M.A. *ISRN Polym. Sci*. **2013**, 1 – 5.
 10. Harisankar, P.; Mohana Reddy, Y.V.; Hemachandra Reddy, K. *Int. Lett. Chem. Phys. Astron*. **2014**, *18*, 75 – 90.
 11. Agubra, V.A.; Owuor, P.S.; Hosur, M.V. *Nanomaterials*. **2013**, *3*, 550 – 563.
 12. Kusmono, Z.A.; Mohd Ishak, Z.A.; Chow, W.S.; Takeichi, T.; Rochmadi, S.U. *Polym. Composite*. **2010**, *31*(7), 1125 – 1308.
 13. Di Pasquale, G.; Pollicino, A. *J. Nanomater*. **2017**, 1 – 11.
 14. Darie, R.N.; Paslaru, E.; Sdrobis, A.; Pricope, G.M.; Hitruc, G.E.; Poiata, A.; Baklavaridis, A.; Vasile, C. *Ind. Eng. Chem. Res*. **2014**, *53*, 7877 – 7890.
 15. Corcione, C.E.; Frigione, M. *Materials*. **2012**, *5*, 2960 – 2980.